ISSN 1996-3343

# Asian Journal of Applied Sciences

http://knowledgiascientific.com

Knowledgia SCIENTIFIC
A Place to Publish Outstanding Research

Asian Journal of Applied Sciences 5 (6): 423-430, 2012
ISSN 1996-3343 / DOI: 10.3923/ajaps.2012.423.430


# Study of Dielectric and Electrical Properties of Nickel Doped Potassium Hexatitanate ($K_2Ti_6O_{13}$) Fine-ceramics

[1]Mohd. Asim Siddiqui, [1]Vishal Singh Chandel and [2]Ameer Azam
[1]Department of Physics, Integral University, Kursi Road, Lucknow-226026, Uttar Pradesh, India
[2]Department of Applied Physics Centre of Excellence in Material Science (Nanomaterials), Z.H. College of Engineering and Technology, Aligrah Muslim University, Aligarh-202002, Uttar Pradesh, India

*Corresponding Author: Mohd. Asim Siddiqui, Department of Physics, Integral University, Kursi Road, Lucknow-226026, Uttar Pradesh, India*

## ABSTRACT

Pure and nickel doped (x = 0.05, 0.10, 0.15 mol%) polycrystalline potassium hexatitanate ($K_2Ti_6O_{13}$) ceramics were synthesized using conventional solid state reaction route. Lattice constants have been evaluated from XRD data recorded at Room Temperature (RT), revealed its single phase formation in a monoclinic symmetry. XRD result corroborated the successful doping of Ni in the $K_2Ti_6O_{13}$ matrix. Dielectric and electrical properties (relative permittivity $\varepsilon'$, loss tangent $\tan\delta$ and ac conductivity $\sigma_{ac}$) have also been studied as a function of frequency at room temperature for all specimens and it is found that these parameters generally decrease with increase in frequency and dopant concentration.

**Key words:** Potassium hexatitanate, solid state reaction route, dielectric constant

## INTRODUCTION

Titanium oxide has attracted attention of researchers considerably due to its potential applications in various fields such as in solar cells (Barbe *et al*., 1997), electronics (Croce *et al*., 1998), photocatalysis (Hodos *et al*., 2004) and sensors (Mor *et al*., 2004). Photocatalytic degradation using semiconductors as catalysts have been shown as the most promising method for the destruction of pollutants in water (Fujishima *et al*., 2000). Among the semiconductor catalysts, $TiO_2$ is the most used photocatalyst showing a high performance such as degradation of Rhodamine B in the presence of $TiO_2$ powder and nanotubes (Pang *et al*., 2010), removal of arsenic from contaminated water by iron based titanium dioxide (Halim *et al*., 2008), photocatalytic activity over methyl orange dye (Fathima *et al*., 2009), photocatalytic degradation of β-naphthol (Qourzal *et al*., 2006), photocatalysis of phenolic compounds (Khuanmar *et al*., 2007), photocatalytic degradation of phenol (Zulfakar *et al*., 2011), removal of colour from landfill by solar photocatalytic (Makhtar *et al*., 2010). It has been observed that besides, $TiO_2$, materials containing titanium oxide have wide applications in various fields. Among such materials alkali titanate family, $M_2Ti_6O_{13}$ (M = Na, Li, K), is the most useful. Conventionally these materials are prepared by solid state reaction method using titanium oxide ($TiO_2$) as a raw material and have interesting technological applications such as ceramic capacitors (Xu *et al*., 2005), dielectric sensors and biosensors (Dominko *et al*., 2006), biophysics and nanotechnology (Becker *et al*., 2007; Wang *et al*., 2003) ion exchange (Bavykin and Walsh, 2007) and photocatalysis (Stengl *et al*., 2006; Teshima *et al*., 2008). $K_2Ti_nO_{2n+1}$, with $3<n<6$, have a wide band gap of about 3.45 eV while that of $TiO_2$ has 3.22 eV and

thus $K_2Ti_6O_{13}$ shows semiconducting behaviour, it is also known for its catalytic activity (Sayama and Arakawa, 1994). Other applications of $K_2Ti_6O_{13}$ are reinforcements for metals, such as copper, to improve their wear resistance (Murakami and Matsui, 1996), plastics to improve their mechanical and dielectric properties (Yu *et al*., 2000) and automotive brake lining pad as a substitute for cancerogenic asbestos (Choy and Han, 1998). Luo *et al*. (2011) reported the mechanical and thermal insulating properties of resin-derived carbon foams reinforced by $K_2Ti_6O_{13}$ whiskers. Physicochemical properties of ambient-dried $SiO_2$ aerogels with $K_2Ti_6O_{13}$ whisker have been investigated (Zhang *et al*., 2009). Physical properties of such compounds may be modified by doping aliovalent 3D transition-metal ions. Recently, effect of Na-substitution on the dielectric behaviour of layered $K_{2-x}Na_xTi_4O_9$ ($0.05 \le x \le 0.15$) ceramics (Vikram *et al*., 2009), structural and dielectric properties of Cu-doped $K_2Ti_6O_{13}$ (Vikram, 2010) have also been reported by our research group. Besides bulk material, preparation and photocatalytic activity of nanomaterials of these pure alkali titanates $M_2Ti_nO_{2n+1}$ (M = Li, Na, K etc.) and silver hexatitanates have also been reported (Song *et al*., 2007; Rodriguez-Gonzalez *et al*., 2009). In the present study synthesis, room temperature dielectric and electrical properties of pure and Ni doped $K_2Ti_6O_{13}$ have been investigated.

## MATERIALS AND METHODS

**Synthesis:** $K_2Ti_6O_{13}$ (PTO) ceramic was prepared by conventional solid-state route taking stoichiometric amounts of the grinded AR grade $K_2CO_3$ and $TiO_2$ powders (purity 99.9%), under acetone and calcined at 1000°C for 24 h followed by furnace cooling. To prepare nickel doped (x = 0.05, 0.10,0.15 mol%) specimens, desired amount of NiO powder (purity 99.9%; AR grade) was added to the mixture of potassium carbonate and $TiO_2$ and the mass so obtained was recycled through the above process. The obtained powder was pressed into pellets of 13 mm diameter and 1.00 mm thickness which were further sintered at 1000°C for 1 h.

**Characterization:** Structural properties of all the specimens were studied by X-Ray Diffraction (XRD) spectrum on a X-ray powder diffractometer using Cu-Kα radiations ($\lambda$ = 0.15406 nm) in 2θ range from 10-70° with scan rate of 2° $min^{-1}$ at room temperature. The Lattice parameters were calculated using relation:

$$\frac{1}{d^2} = \frac{h^2}{a^2 \sin^2\beta} + \frac{k^2}{b^2} + \frac{l^2}{c^2 \sin^2\beta} - \frac{2hl\cos\beta}{ac\sin^2\beta} \quad (1)$$

The dielectric and electrical measurements were carried out after applying the silver paste on the flat faces of the pellets, in the frequency range 100-1000 KHz using LCR HI-Tester (HIOKI 3532-50). The value of dielectric constant ($\varepsilon_r$) is calculated using the formula:

$$\varepsilon_r = \frac{C_p \times d}{\varepsilon_0 \times A} \quad (2)$$

where, $\varepsilon_0$ is the permittivity of free space, d is thickness of pellet, A is the cross-sectional area of the flat surface of the pellet and $C_p$ is the capacitance of the specimen in Farad (F).

The complex dielectric constant (ε") of all the samples were calculated using the relation:

$$\varepsilon'' = \varepsilon_r \tan\delta \quad (3)$$

where, tanδ is the dielectric loss tangent, proportional to the loss of energy from the applied field into the sample (this energy is dissipated as heat) and therefore denoted as dielectric loss.

The ac conductivity of the samples was determined using the relation:

$$\sigma_{ac} = \varepsilon_r \varepsilon_0 \omega \tan\delta \quad (4)$$

where, ω is the angular frequency and tanδ denotes the dielectric loss tangent.

## RESULTS AND DISCUSSION

**Structural properties:** Figure 1 shows the XRD patterns, achieved at RT, for pure and nickel doped (x = 0.0, 0.05, 0.10, 0.15) $K_2Ti_6O_{13}$ ceramics. Further, no other impurity peak was observed in the XRD pattern showing the single phase sample formation. The peak position of each sample exhibits the monoclinic crystal symmetry which was confirmed from ICDS card No. 74-0275. The variations in the lattice parameters and cell volume have also been studied for different doping concentrations and presented in Table 1. The unit cell parameters reported by other researcher (Vikram, 2010) fairly coincides with the calculated values. The ionic radius of $Ni^{2+}$ is 72 pm whereas that of $Ti^{4+}$ is 68 pm. The Ni ions substitute the $Ti^{4+}$ ions in the crystal due to comparable ionic radius. However, the increase in the lattice parameter may be due to the larger ionic radius of Ni ions. Hence, we can observe that doping invariably and consistently expands the unit cell volume.

Table 1: List of pure and nickel doped $K_2Ti_6O_{13}$ ceramic samples with unit cell volume and lattice parameters

| | Ni-doping lattice parameters | | | | |
|---|---|---|---|---|---|
| | a (Å) | b (Å) | c (Å) | β (degree) | Unit cell volume (Å$^3$) |
| x = 0.00 | 15.570 | 3.806 | 9.104 | 99.568 | 531.90 |
| x = 0.05 | 15.587 | 3.819 | 9.162 | 99.667 | 537.60 |
| x = 0.10 | 15.610 | 3.834 | 9.174 | 99.723 | 541.10 |
| x = 0.15 | 15.655 | 3.835 | 9.200 | 99.874 | 544.10 |

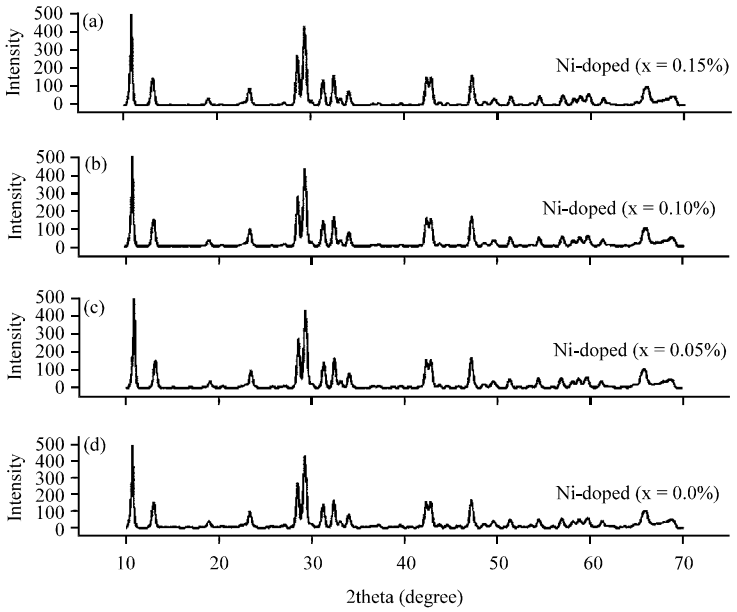


Fig. 1(a-d): XRD patterns for pure and nickel doped $K_2Ti_6O_{13}$ ceramics

If we consider the schematic structure of $K_2Ti_6O_{13}$, it may be described having $K^+$ ions in the tunnel space contributing in the ionic conduction while $TiO_6$ (or $NiO_6$) assembly is attached with each other forming zigzag ribbons joined by edge-sharing (Xie and Lu, 2003).

**Dielectric properties:** The dielectric constant is represented by $\varepsilon = \varepsilon_r - i\varepsilon''$ where $\varepsilon_r$ is real part of dielectric constant (relative permittivity) and describes the stored energy while $\varepsilon''$ is imaginary part of dielectric constant which describes the dissipated energy. Figure 2a shows the frequency response of dielectric constant, recorded at RT, in the frequency range of 100-1000 kHz for x = 0.0, 0.05, 0.10 and 0.15, respectively. It is clear from the figure that dielectric constant decreases with the increase in frequency for all samples and this type of behavior can be explained on the basis of Maxwell-Wagner model (Prodromakis and Papavassiliou, 2009). According to this model, a dielectric medium is assumed to be made of well conducting grains which are separated by poorly conducting (or resistive) grain boundaries. Under the application of external electric field, the charge carriers can easily migrate the grains but are accumulated at the grain boundaries. This process can produce large polarization and high dielectric constant. The small conductivity of grain boundary contributes to the high value of dielectric constant at low frequency. The dielectric constant decreases with frequency as various polarisation processes ceases at higher frequencies. It has also been observed that the value of dielectric constant decreases with the increase in Ni dopant. It may be due to the small dielectric polarizability of nickel ions (1.23 $Å^3$) compared to titanium ion (2.93 $Å^3$) (Shannon, 1993). Hence, as the dopant concentration increases more titanium ions will be substituted by nickel ions and thereby decreasing the dielectric polarization which in turn decreases the dielectric constant.

Figure 2b shows the frequency response of dielectric loss, achieved at RT, in the frequency range of 100-1000 kHz for x = 0.0, 0.05, 0.10 and 0.15, respectively. We can mark the exponential demise of losses for all the ceramic specimens. However, losses decrease exponentially with the application of ac field owing to the fact that at higher frequencies, ceramic specimens offer low reactance to the sinusoidal signal and hence minimize the conduction losses (Bogoroditsky *et al.*, 1979). Therefore, dielectric losses decrease at higher frequency. These types of variations in the dielectric losses are characteristic of the dipole orientation and electrical conduction (Lingwal *et al.*, 2003). Doping concentration x = 0.10 increases dielectric losses to very high values as compared to x = 0. 05 and x = 0.0. However, further doping causes the decrease in losses to a significant limit. For heavy doping (x = 0.15) any further, dielectric losses are decreased to very low values even below the values for undoped sample (x = 0). Similar behavior of dielectric constant and loss tangent is also reported by Mahato *et al.* (2006) for $Pb_{1-3x/2}\ Sm_x\ (Zr_{.53}\ Ti_{.47})O_3$ ceramic system.

**Electrical investigation:** Figure 2c shows the room temperature frequency response of ac conductivity in the range of 100-1000 kHz for x = 0.0, 0.05, 0.10 and 0.15, respectively. The ac conductivity increases with the increase in frequency for all compositions. It has been observed that ac conductivity gradually increases with the increase in frequency of applied ac field because the increase in frequency enhances the electron hopping frequency. It can also be seen from Fig. 2c that conductivity increases with the increase in dopant concentration up to 10% and then decreases for 15%. It may be attributed to the fact that the dopants of $Ni^{2+}$ are acceptors for $K_2Ti_6O_{13}$ and are usually compensated by the formation of oxygen vacancies. Thus, the increase in dopant concentration increases the oxygen vacancies which results in an increase of free electron density and conductivity. However, the substitution of $Ti^{4+}$ with $Ni^{2+}$ can take place up to a certain limit.

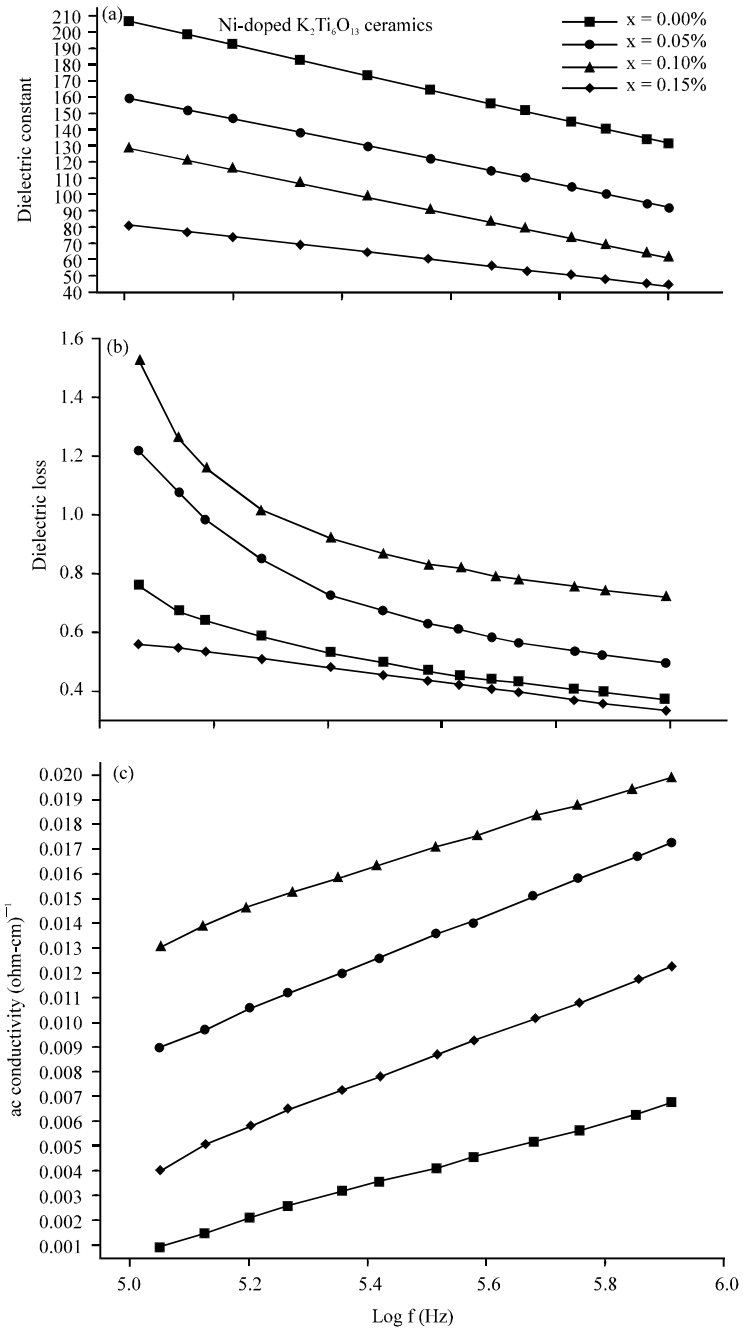


Fig. 2(a-c): (a)Variation of real dielectric constant with frequency for $K_2Ti_6O_{13}$ and its nickel doped derivatives, (b) Variation of loss tangent with frequency for $K_2Ti_6O_{13}$ and its nickel doped derivatives and (c) Variation of ac conductivity with frequency for $K_2Ti_6O_{13}$ and its nickel doped derivatives

When the introduction of $Ni^{2+}$ exceeds this limit, the superfluous $Ni^{2+}$ which cannot substitute $Ti^{4+}$ further will segregate to grain boundary interfaces. Thus, the segregation of $Ni^{2+}$ blocks the building and transportation of electrons and other defects and thereby decreases the conductivity.

## CONCLUSION

$K_2Ti_6O_{13}$ and its nickel doped (x = 0.05, 0.10, 0.15 mol%) ceramic specimens were synthesized using solid-state route. Lattice constants evaluated from room temperature XRD spectra revealed the phase formation in a monoclinic symmetry. Lattice constant have been found to increase with the increase in nickel concentration. The data revealed that the dielectric constant exhibit the normal dielectric behaviour and decrease with the increase in frequency and dopant concentration. Due to variation of doping concentration dielectric loss was primarily found to increase due to space charges but further it decreases due to inhibition of domain-wall motion. The ac conductivity shows the frequency and composition dependent behaviour. It increases with the increase in frequency and dopant concentration.

## ACKNOWLEDGMENT

Authors are thankful to the Council of Science and Technology, Govt. of UP, India for the financial support in the form of centre of excellence in material science (nanomaterials), A.M.U., Aligarh, India.

## REFERENCES

Barbe, C.J., F. Arendse, P. Comte, M. Jirousek, F. Lenzmann, V. Shklover and M. Gratzel, 1997. Nanocrystalline titanium oxide electrodes for photovoltaic applications. J. Am. Ceram. Soc., 80: 3157-3171.

Bavykin, D.V. and F.C. Walsh, 2007. Kinetics of alkali Metal ion exchange into nanotubular and nanofibrous titanates. J. Phys. Chem. C., 111: 14644-14651.

Becker, I., I. Hofmann and F.A. Muller, 2007. Preparation of bioactive sodium titanate ceramics. J. Eur. Ceram. Soc., 27: 4547-4553.

Bogoroditsky, N.P., V.V. Pasynkov and B. Tareev, 1979. Electrical Engineering Materials. Mir Publishers, Moscow, Russia.

Choy, J.H. and Y.S. Han, 1998. A combinative flux evaporation-slow cooling route to potassium titanate fibres. Mater. Lett., 34: 111-118.

Croce, F., G.B. Appetecchi, L. Persi and B. Scrosati, 1998. Nanocomposite polymer electrolytes for lithium batteries. Nature, 394: 456-458.

Dominko, R., E. Baudrin, P. Umek, D. Arcon, M. Gaberscek and J. Jamnik, 2006. Reversible lithium insertion into $Na_2Ti_6O_{13}$ structure. Electrochem. Commun., 8: 673-677.

Fathima, I., P.R. Shukla and F. Kooli, 2009. Combined photocalytic and fenton oxidation of methyl orange dye using iron exchange titanium pillared montmorillonite. J. Applied Sci., 9: 3715-3722.

Fujishima, A., T.N. Rao and D.A. Tryk, 2000. Titanium dioxide photocatalysis. J. Photochem. Photobiol. C: Photochem. Rev., 1: 1-21.

Halim, M.A., S. Safiullah, M.S. Rana and M.A. Goni, 2008. Removal of arsenic from contaminated water by iron based titanium-dioxide from beach sand. Res. J. Environ. Sci., 2: 498-502.

Hodos, M., E. Horvath, H. Haspel, A. Kukovecz, Z. Konya and I. Kiricsi, 2004. Photosensitization of ion exchangeable titanate nanotubes by CdS nanoparticles. Chem. Phys. Lett., 399: 512-515.

Khuanmar, K., W. Wirojanagud, P. Kajitvichyanukul and S. Maensiri, 2007. Photocatalysis of phenolic compounds with synthesized nanoparticles $TiO_2$/$Sn_2$. J. Applied Sci., 7: 1968-1972.

Lingwal, V., B.S. Semwal and N.S. Panwar, 2003. Dielectric properties of $Na_{1-x}K_xNbO_3$ in orthorhombic phase. Bull. Mater. Sci., 26: 619-625.

Luo, R., Y. Ni, J. Li, C. Yang and S. Wang, 2011. The mechanical and thermal insulating properties of resin-derived carbon foams reinforced by $K_2Ti_6O_{13}$ whiskers. Materials Sci. Eng. A., 528: 2023-2027.

Mahato, D.K., 2006. Dielectric behavior of $Pb_{1-3x/2}$ $Sm_x$ $(Zr_{0.53}$ $Ti_{0.47})O_3$ ceramic system. J. Applied Sci., 6: 716-720.

Makhtar, S.M.Z., N. Ibrahim and M.T. Selimin, 2010. Removal of colour from landfill by solar photocatalytic. J. Applied Sci., 10: 2721-2724.

Mor, G.K, M.A. Carvalho, O.K. Varghese, M.V. Pishko and C.A. Grimes, 2004. A room-temperature $TiO_2$ nanotube hydrogen sensor able to self-clean photoactively from environmental contamination. J. Mater. Res., 19: 628-634.

Murakami, R. and K. Matsui, 1996. Evaluation of mechanical and wear properties of potassium acid titanate whisker-reinforced copper matrix composites formed by hot isostatic pressing. Wear, 201: 193-198.

Pang, Y.L., A.Z. Abdullah and S. Bhatia, 2010. Comparison of sonocatalytic activities on the degradation of rhodamine B in the presence of $TiO_2$ powder and nanotubes. J. Applied Sci., 10: 1068-1075.

Prodromakis, T. and C. Papavassiliou, 2009. Engineering the Maxwell-Wagner polarization effect. Applied Surf. Sci., 255: 6989-6994.

Qourzal, S., M. Tamimi, A. Assabbane, A. Bouamrane, A. Nounah, L. Laanab and Y. Ait-Ichou, 2006. Preparation of $TiO_2$ photocatalyst using $TiCl_4$ as a precursor and its photocatalytic performance. J. Applied Sci., 6: 1553-1559.

Rodriguez-Gonzalez, V., M.A. Ruiz-Gomez, L.M. Torres-Martinez, R. Zanella and R. Gomez, 2009. Sol gel silver hexatitanates as photocatalysts for the 4-chlorophenol decomposition. Catalysis Today, 148: 109-114.

Sayama, K. and H. Arakawa, 1994. Effect of $Na_2CO_3$ addition on photocatalytic decomposition of liquid water over various semiconductor catalysis. J. Photochem. Photobiol. A Chem., 77: 243-247.

Shannon, R.D., 1993. Dielectric polarizabilities of ions in oxides and fluorides. J. Applied Phys., 73: 348-366.

Song, H., H. Jiang, T. Liu, X. Liu and G. Meng, 2007. Preparation and photocatalytic activity of nanomaterials $A_2Ti_nO_{2n+1}$. Mater. Res. Bull., 42: 334-344.

Stengl, V., S. Bakardjieva, J. Subrt, E. Vecernikova and L. Szatmary, *et al.*, 2006. Sodium titanate nanorods: Preparation, microstructure characterization and photocatalytic activity. Appl. Catal. B, Environ., 63: 20-30.

Teshima, K., K. Yubuta, T. Shimodaira, T. Suzuki, M. Endo, T. Shishido and S. Oishi, 2008. Environmentally friendly growth of highly crystalline photocatalytic $Na_2Ti_6O_{13}$ whiskers from NaCl flux. Cryst. Growth Des., 8: 465-469.

Vikram, S.V., 2010. Structural and electrical properties of Cu doped $K_2Ti_6O_{13}$. J. Alloys Compounds, 489: 700-707.

Vikram, S.V., D. Maurya and V.S. Chandel, 2009. Effect of Na-Substitution on the dielectric behaviour of layered $K_{2-x}Na_xTi_4O_9$ $(0.05 \leq x \leq 0.15)$ ceramics. J. alloys and Compounds. 478: 398-403.

Wang, B.L., Q. Chen, R.H. Wang and L.M. Peng, 2003. Synthesis and characterization of $K_2Ti_6O_{13}$ nanowires. Chem. Phys. Lett., 376: 726-731.

Xie, J. and X. Lu, 2003. AFM study on potassium hexatitanate whiskers. J. Material Sci., 38: 3641-3646.

Xu, C.Y., Q. Zhang, H. Zhang, L. Zhen, J. Tang and L.C. Qin, 2005. Synthesis and characterization of single-crystalline alkali titanate nanowires. J. Am. Chem. Soc., 127: 11584-11585.

Yu, D., J. Wu, L. Zhou, D. Xie and S. Wu, 2000. The dielectric and mechanical properties of potassium titanate-whisker-reinforced PP/PA blend. Compos. Sci. Technol., 60: 499-508.

Zhang, H., X. He and F. He, 2009. Microstructure and physicochemical properties of ambient dried $SiO_2$ aerogels with $K_2TI_6O_{13}$ whisker additive. J. Alloys Compounds, 472: 194-197.

Zulfakar, M., N.A.H. Hairul, H.M.R. Akmal and M.A. Rahman, 2011. Photocalytic degradation of phenol in a fluidized bed reactor using immobilized $TiO_2$ photocatalyst. J. Applied Sci., 11: 2320-2326.